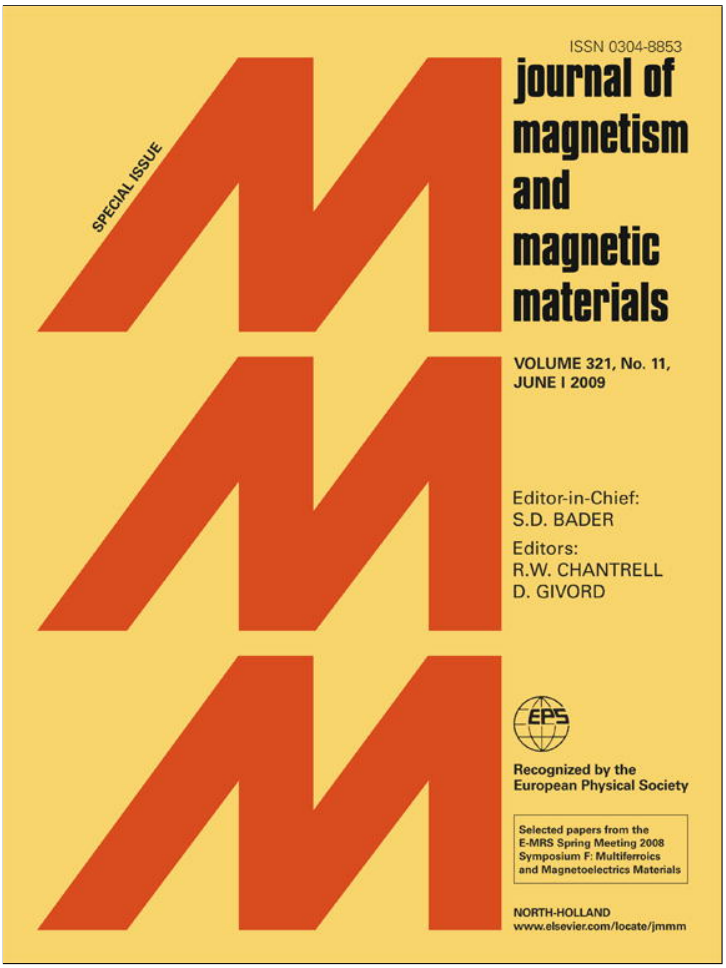

Journal of Magnetism and Magnetic Materials 321 (2009) 1739–1742

Contents lists available at ScienceDirect

Journal of Magnetism and Magnetic Materials

journal homepage: www.elsevier.com/locate/jmmm

Magnetoelectric behavior in the complex $CaMn_7O_{12}$ perovskite

M. Sánchez-Andújar [a], S. Yáñez-Vilar [a], N. Biskup [b], S. Castro-García [a], J. Mira [c], J. Rivas [c], M.A. Señarís-Rodríguez [a,*]

[a] Departamento Química Fundamental, Facultad de Ciencias Universidade da Coruña, 15071 A Coruña, Spain
[b] Instituto de Ciencias de Materiales, CSIC, Cantoblanco, 28049 Madrid, Spain
[c] Dpto. Física Aplicada, Universidade de Santiago de Compostela, 15782 Santiago de Compostela, Spain

ARTICLE INFO

Available online 11 February 2009

PACS:
77.22.−d
75.90.+w
61.10.Nz

Keywords:
Magnetoelectric
Perovskite
Charge-ordering

ABSTRACT

We report a magnetoelectric effect in the double perovskite $CaMn_7O_{12}$, that shows a complex magnetic behavior below 90 K with two magnetic phases coexisting (one ferrimagnetic and the other modulated). A second magnetic transition, associated with changes in the magnetic modulation and magnetic ordering coherence lengths of the two magnetic phases occurs at 50 K (T_{N2}). A detailed structural characterization of this compound, that we have carried out by means of high-resolution X-ray powder diffraction, reveals an anisotropic thermal expansion of its lattice parameters at 50 K (T_{N2}). In addition, our study of the complex permittivity of this sample as a function of temperature, frequency and magnetic field shows very interesting results below 90 K and specially below 50 K: the dielectric constant ε'_r that was decreasing continuously on cooling experiences an upturn, and even more, on application of a magnetic field it shows a moderate magnetoelectric response. We attribute such dielectric behavior to the formation of electric dipoles by magnetostriction in this charge and spin ordered system, that are sensible to the presence of an external magnetic field.

1. Introduction

In the past years, many efforts have been devoted to the search for new single phase multiferroic compounds, that simultaneously show ferroelectricity and cooperative magnetism and in which both properties couple [1,2] so as to give rise to the cross-phenomenon know as the magnetoelectric (ME) effect. Such property is specially interesting from the application point of view, because it allows the manipulation of the magnetic response with an external electric field and the tuning of the dielectric behavior as a function of the magnetic field in new multifunctional materials.

Although the conventional mechanisms that allow ferroelectricity and ferro/antiferromagnetism are mutually exclusive [3], new alternatives have been described that open new routes to new magnetoelectric multiferroic compounds [4].

In this context, the compounds with perovskite structure have indeed attracted the tremendous interest because these materials do display the interesting magnetoelectric effect [5,6].

In this paper, we report the study of a "new" multiferroic material, the $CaMn_7O_{12}$ mixed oxide. This compound is a complex perovskite that presents charge and orbital ordering (CO and OO) at relatively high temperatures [7] and a frustrated magnetic arrangement at low temperatures [8].

From the structural point of view, the compound $CaMn_7O_{12}$ belongs to the $(AA'_3)B_4O_{12}$ family, as it can be more readily seen when formally writing its formula as: $(CaMn_3^{3+})(Mn_3^{3+}Mn^{4+})O_{12}$. This perovskite-derived phase consists of a three-dimensional array of corner sharing $[BO_6]$ octahedra that are tilted, so that one-fourth of the A-sites are distorted into icosahedra (that are occupied by Ca^{2+} ions) and three-fourths into a square–planar coordination that accommodate the Jahn–Teller Mn^{3+} ions. Above 440 K, different manganese ions (formally Mn^{3+} and Mn^{4+}) occupy the octahedral B-sites randomly and the symmetry is cubic (S.G.: $Im\bar{3}$). At 440 K, this compound experiences a structural phase transition associated to the electronic processes of CO and OO and the symmetry becomes trigonal (S.G.: $R\bar{3}$) [9], due to the ordering of the distinguishable Mn^{3+} and Mn^{4+} ions in the B sublattice. In this trigonal structure, the B-site Mn^{3+} ions show a distorted octahedral environment with two different bond lengths, four long and two short distances, typical of a Jahn–Teller distortion with a half-filled $d_{x^2-y^2}$ orbital, and that is very uncommon for perovskite type materials with Mn^{3+} ions [10]. On the other hand, the Mn^{4+} cations are in a regular octahedral enviroment.

Such a crystal structure with comparable Mn (A-site)–O and Mn (B-site)–O bond lengths as well as comparable Mn (A-site)–O–Mn (B-site) and Mn (B-site)–O–Mn (B-site) angles is

* Corresponding author. Tel.: +34 981 167000; fax: +34 981 167065.
E-mail address: tonasr@udc.es (M.A. Señarís-Rodríguez).

0304-8853/$ - see front matter © 2009 Elsevier B.V. All rights reserved.
doi:10.1016/j.jmmm.2009.02.018

specially adequate for the appearance of highly frustrated magnetic arrangements.

In this context this compound, that is paramagnetic above ~90 K, experiences two magnetic transitions at $T \approx 90$ K (T_{N1}) and $T \approx 50$ K (T_{N2}) [8,11]. According to neutron powder diffraction results, on cooling below 90 K and down to 50 K two magnetic phases coexist [8,11]: a ferrimagnetic α-phase and a modulated β-phase. Below 50 K, the ferrimagnetic α-phase becomes modulated and the already modulated β-phase experiences changes in its modulation and magnetic ordering coherent length. In all modulated phases, the modulation propagation vector is parallel to the crystallographic *c*-axis.

In previous works, we have studied the dielectric response of the $CaMn_7O_{12}$ perovskite in the paramagnetic region [12–14] finding that this compound shows a high dielectric constant (~10^6) at room temperature with frequency independent values in a broad temperature range, as the isostructural $CaCu_3Ti_4O_{12}$ perovskite [15]. To explain the observed dielectric response, we have proposed a Maxwell–Wagner relaxation, due to the presence of three electrically different regions in the material [13].

In this work, we have focused on the low temperature range ($T < 100$ K) to study the influence of the magnetic transitions on the dielectric behavior.

2. Experimental

As described elsewhere, we have prepared $CaMn_7O_{12}$ as a polycrystalline material by the Pechini method using $CaCO_3$ (Panreac, >98,6%) and $Mn(NO_3)_2 \cdot H_2O$ (Aldrich, >98%) as starting materials and with a final heating treatment at 975 °C/48 h [13].

The purity of the obtained material was initially checked by conventional X-ray powder diffractometry (XRPD) in a Siemens D-5000 diffractometer and using Cu (Kα) = 1.5418 Å radiation.

In addition, high-resolution synchrotron X-ray powder diffraction (SXRPD) was carried out as a function of temperature ($10 \leqslant T(K) \leqslant 100$) in the ID31 beamline ($\lambda = 0.3994$ Å) at ESRF (Grenoble, France). For this purpose, the sample was loaded in a borosilicate capillary ($\phi = 0.3$ mm) and rotated during data collection. The Rietveld analyses were performed with the GSAS program [16], where the peak shapes were described by a pseudo-Voigt function; the background was modeled with a 10-term polynomial and in the final steps of the refinement all atomic coordinates and isotropic temperature factors were included.

Magnetic properties were studied in a Quantum Design MPMS Squid magnetometer. In this context, zero-field-cooled (ZFC) and field-cooled (FC) magnetic susceptibility data were obtained under a field of 1000 Oe in the temperature range $5 \leqslant T(K) \leqslant 300$.

The relative complex permittivity of this sample, $\varepsilon_r(\omega) = \varepsilon'_r(\omega) - i\varepsilon''_r(\omega)$, was measured with a precision LCR-meter Quadtech model 1920 capable to measure in frequencies ranging from 20 to 10^6 Hz in the temperature range ($5 < T(K) < 100$) and under the magnetic field up to 10 T. To ensure a good electrical contact gold was sputtered on the surfaces of the pelletized sample.

Impedance complex plane plots were analysed using the LEVM program [17].

3. Results and discussion

3.1. General characterization

According to the conventional X-ray powder diffraction results, $CaMn_7O_{12}$ is the major phase present in the sample, although the presence of weak extra peaks reveals the presence of small amounts of Mn_3O_4 (hausmanite). Quantitative analysis by the Rietveld method of both the XRD and the SXRPD data indicate that this impurity is present in a very small amount: <2%.

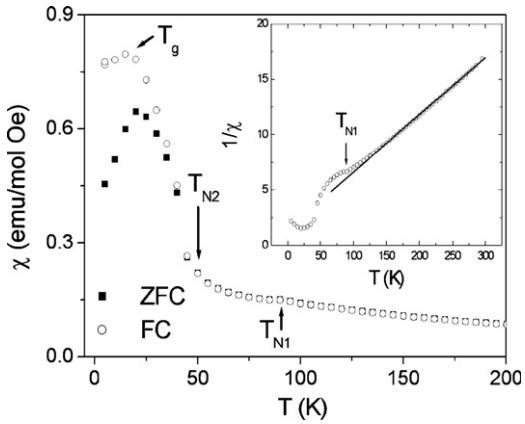

Fig. 1. (a) Field-cooled (FC) susceptibility vs. temperature ($5 < T(K) < 200$). Inset: inverse susceptibility vs. temperature curve under a magnetic field of 1000 Oe.

In order to check its quality, we studied its magnetic properties to confirm that it shows the transitions reported in the literature for this compound [8,18].

In Fig. 1, we show the temperature dependence of the ZFC and FC susceptibility of this sample, results that are similar to those reported by other authors [8,18]. As expected, a small kink appears at the antiferromagnetic ordering temperature, T_{N1}~90 K; mean while at T_{N2}~50 K the susceptibility markedly increases and the FC and ZFC curves split.

3.2. Detailed structural characterization

In the whole temperature range studied ($10 \leqslant T(K) \leqslant 100$), the SXRPD patterns were refined in a trigonal symmetry (S.G: $R\bar{3}$) (Fig. 2). The obtained lattice parameters, refined atomic coordinates, agreement factors and interatomic distances are consistent with the data available in the literature for this compound [10].

Fig. 3 shows the evolution of the obtained cell parameters and volume as a function of temperature. As it can be seen at ≈ 50 K (T_{N2}), the *a* parameter and the cell volume go through a minimum, while the *c* parameter reaches a maximum. Such anomaly in the *a* and *c* cell parameters had been previously reported by Przenioslo et al. [10], even if these authors did not observe any anomaly in the cell volume. These results seem to indicate that the magnetic transition at 50 K is coupled to the lattice inducing a magnetostriction effect.

3.3. Dielectric properties

In contrast to the very high values displayed by the dielectric constant of $CaMn_7O_{12}$ at higher temperatures [11], for $T < 100$ K it shows much lower values $\varepsilon'_r \approx 25$ (Fig. 4a) that are frequency independent.

To deepen further into the dielectric behavior of this compound, we have performed impedance complex plane (Z'' vs. Z') analysis [19] of the obtained data. Typical impedance complex plane plots show a single large arc that can be modelled by a resistance (R), a capacitance (C) and a frequency-dependent distributed element (DE) connected in parallel. As this arc goes to zero and the order of magnitude of the corresponding C is of pF cm^{-1}, it means that only the intrinsic response of the bulk material is observed in this temperature range.

As temperature decreases from 100 to 50 K the dielectric constant is seen to smoothly decrease, and no anomalies are

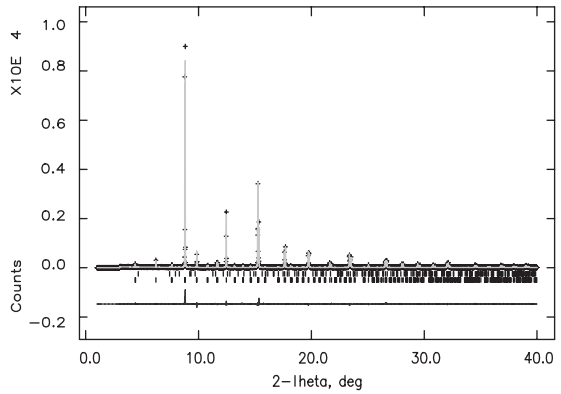

Fig. 2. Rietveld refinement of the SXRPD pattern of $CaMn_7O_{12}$ at $T = 10$ K. Key: observed data (+) and calculated profile (solid line); the difference plot is drawn below the profile. Lower tick marks indicate peak positions of the $CaMn_7O_{12}$ sample and upper tick marks Mn_3O_4 sample.

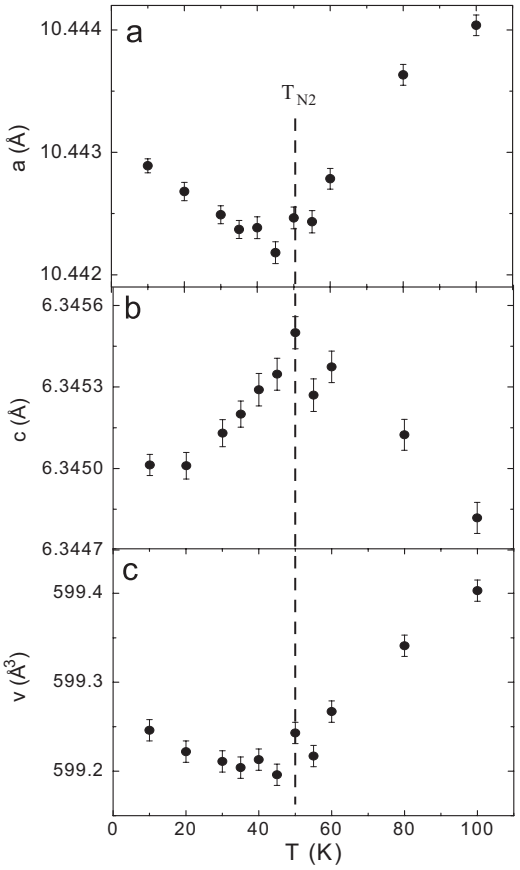

Fig. 3. Evolution of the cell parameters and the cell volume of $CaMn_7O_{12}$ as a function of temperature according to the SXRPD data.

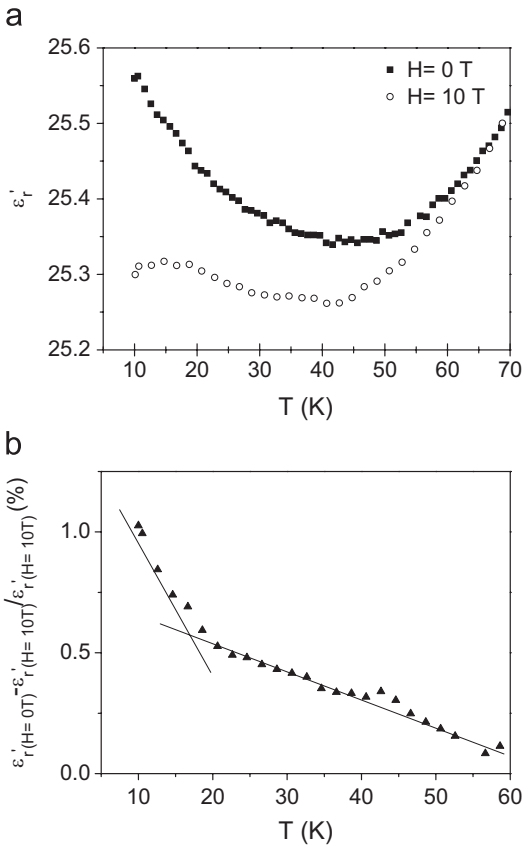

Fig. 4. (a) Temperature dependence of the dielectric constant measured at $\nu = 8000$ Hz below $T = 70$ K and (b) magnetodielectric effect observed at $\nu = 8000$ Hz below $T = 60$ K and expressed as $ME = [\varepsilon'_{r(H=0T)} - \varepsilon'_{r(H=10T)}]/\varepsilon'_{r(H=10T)}$.

detected at $T_{N1} \approx 90$ K, temperature of formation of the ferrimagnetic α-phase and a modulated β-phase.

Meanwhile, after crossing $T_{N2} \approx 50$ K the temperature dependence of the dielectric constant is seen to change and ε'_r experiences an upturn as temperature decreases further (Fig. 4a). Such an increase cannot be due to a classical transition to a ferroelectric state as no structural transitions are detected below 100 K neither in our structural studies nor in those performed by other authors [9].

Another very interesting point is that for $T < 60$ K the dielectric constant of $CaMn_7O_{12}$ is seen to decrease upon application of a magnetic field, and this magnetoelectric effect is more pronounced below 20 K (see Fig. 4b). In any case, such effect is relatively small $ME = [\varepsilon'_{r(H=0T)} - \varepsilon'_{r(H=10T)}]/\varepsilon'_{r(H=10T)} \sim 1\%$ at $T = 10$ K under a magnetic field of 10 T.

To understand the origin of such a dielectric behavior and magnetoelectric effect—that cannot be attributed to the presence of the Mn_3O_4 impurity, as their behaviors are very different [20]. We have to take into account the strong interplay between spin, orbital, lattice and charge degrees of freedom in this compound, as reflected, for example in the magnetostriction effect observed below 50 K.

For this purpose and using the information available in the literature [11], we represent in Fig. 5 the magnetic arrangement present in this compound for $T < 50$ K. As it can be observed, along the *c*-axis the magnetic moments of the manganese cations are ferromagnetically aligned; meanwhile along the {−111} direction, the α-chains with all the Mn cations in the trivalent state show a spin structure up/up/down/down and the β-chains, with alternating Mn^{+3} and Mn^{+4} cations show a spin structure up/up/down/down.

According to very recent theoretical predictions of the β-chains of this structure, Van den Brink and Khomskii [21] present all the necessary ingredients for the appearance of polarization induced by magnetostriction in charge and spin ordered systems.

We suggest that such a mechanism [21] would be acting in this compound: Magnetostriction that occurs at 50 K and that is known to be different for ferro and antiferro bonds, would cause bond alternation that in turn would give rise to the formation of electric dipoles and the observed upturn of the dielectric constant below 50 K.

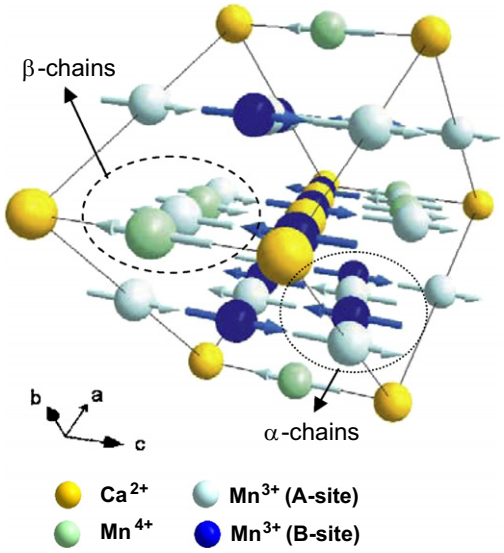

Fig. 5. Magnetic arrangement present in $CaMn_7O_{12}$ as reconstructed from the data available in the literature.

When a magnetic field is applied, the competition between the internal field and the applied field provokes the destruction of polar entities, therefore the dielectric constant is no longer enhanced below T_{N2} and a positive magnetoelectric response is observed. More work on this compound, both experimental and theoretical, is needed to completely clarify the interesting magnetoelectric effect is described here. Specially, the study of single crystals or thin films will be very important.

Acknowledgments

The authors are grateful from financial support for MEC (Spain) under project FEDER MAT 2007-66696 and Xunta de Galicia under project PGIDIT06PXB103298PR. S. Yáñez-Vilar want to thank to MEC of Spain for her FPI fellowship and M. Sánchez-Andújar acknowledges to Xunta de Galicia for support under program Parga Pondal. We also acknowledge the European Synchrotron Radiation Facility for provision of synchrotron radiation facilities and we would like to thank Michela Brunelli for his assistance in using beamline ID31.

References

[1] M. Fiebig, J. Phys. D: Appl. Phys. 38 (2005) R123.
[2] W. Eerenstein, N.D. Mathur, J.F. Scott, Nature 442 (2006) 759.
[3] N.A. Hill, J. Phys. Chem. B 104 (2000) 6694.
[4] S.W. Cheong, M. Mostovoy, Nat. Mater. 6 (2007) 13.
[5] W. Prellier, M.P. Singh, P. Murugavel, J. Phys.: Condens. Matter 17 (2005) R803.
[6] D.I. Khomskii, J. Magn. Magn. Mater. 306 (2006) 1.
[7] I.O. Troyanchuk, A.N. Chobot, Crystallogr. Rep. 42 (1997) 983.
[8] R. Przenioslo, I. Sosnowska, D. Hohlwein, T. Hauβ, I.O. Troyanchuk, Solid State Commun. 111 (1999) 687.
[9] B. Bochu, J.L. Buevoz, J. Chenavas, A. Collomb, J.C. Joubert, M. Marezio, Solid State Commun. 36 (1980) 133.
[10] R. Przenioslo, I. Sosnowska, E. Suard, A. Hewat, A.N. Ficht, Physica B 344 (2004) 358.
[11] R. Przenioslo, I. Sosnowska, E. Suard, T. Hansen, Appl. Phys. A 74 (2002) S1731.
[12] A. Castro–Couceiro, S. Yáñez–Vilar, B. Rivas–Murias, A. Fondado, J. Mira, J. Rivas, M.A. Señarís–Rodríguez, J. Phys.: Condens. Matter 18 (2006) 3803.
[13] S. Yáñez–Vilar, A. Castro–Couceiro, B. Rivas–Murias, A. Fondado, J. Mira, J. Rivas, M.A. Señarís–Rodríguez, Z. Anorg. Allg. Chem. 631 (2005) 2192.
[14] A. Castro–Couceiro, S. Yáñez–Vilar, M. Sánchez–Andujar, B. Rivas–Murias, J. Rivas, M.A. Señaris–Rodriguez, Prog. Solid State Chem. 35 (2007) 379.
[15] M.A. Subramanian, D. Li, N. Duan, B.A. Reisner, A.W. Sheight, J. Solid State Chem. 151 (2000) 323.
[16] A.C. Larson, R.B. von Dreele, General Structure Analysis System (GSAS), Los Alamos National Laboratories, Report LAUR (1990) 86.
[17] J. Ross Macdonald, LEVM version 8.0 Complex Nonlinear Squares Fitting Program (2003).
[18] O. Volkova, Y. Arango, N. Tristan, V. Kataev, E. Gudilin, D. Meier, T. Lorenz, B. Büchner, A. Vasilev, JETP Lett. 82 (2005) 444.
[19] J. Ross Macdonald, Impedance Spectroscopy: Emphasizing Solid Materials and Systems, Wiley, New York, 1987.
[20] R. Tackett, G. Lawes, B.C. Melot, M. Grossman, E.S. Toberer, R. Seshadri, Phys. Rev. B 024409 (2007).
[21] J. van den Brink, D.I. Khomskii, J. Phys.:Condens. Matter 20 (2008) 434217.